Supporting Figures

Ren L, et al. Fig. S1

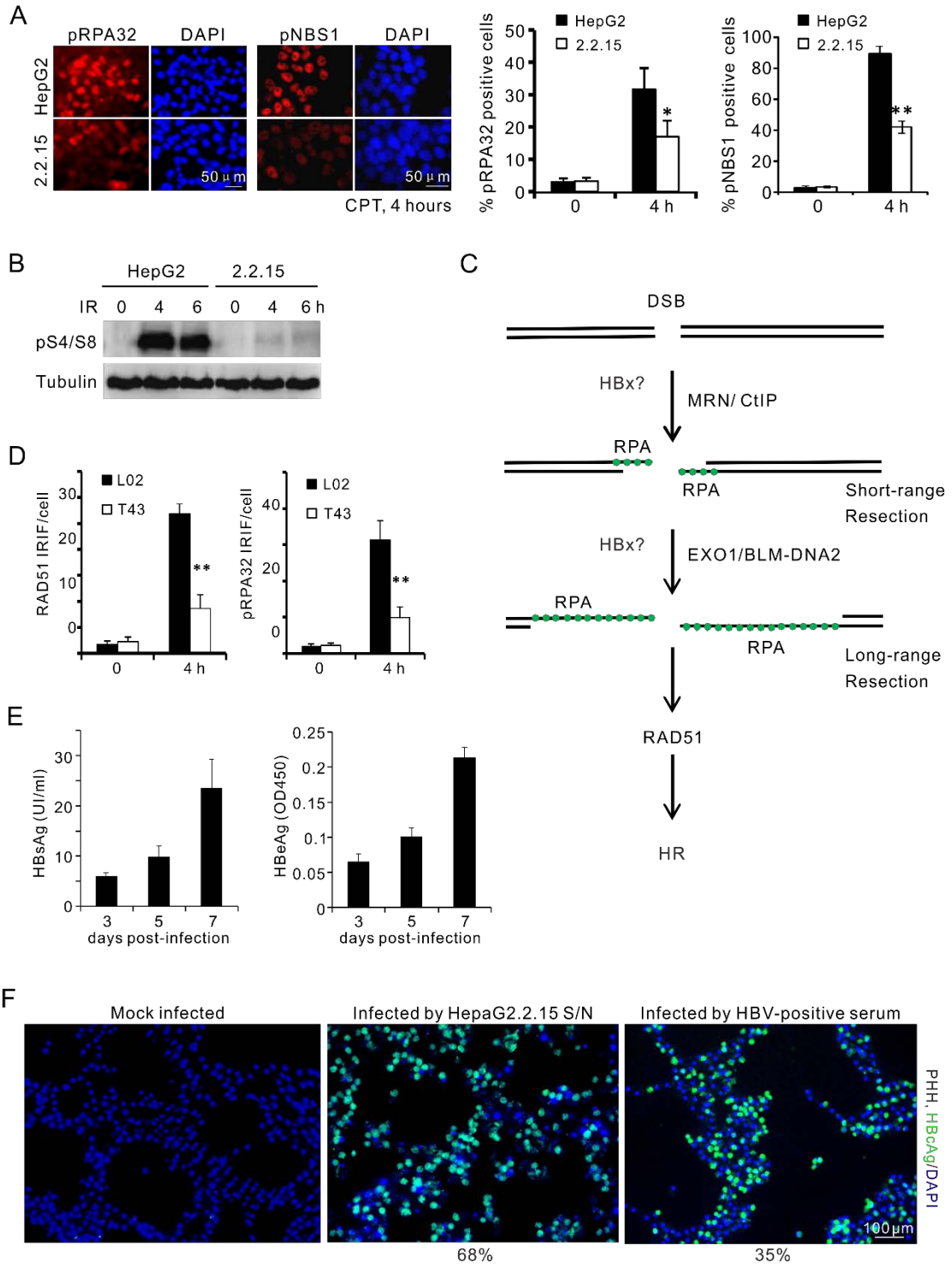

Fig.S1 (A) Pan-nuclear phosphorylation of RPA32 (pSerine 33) and NBS1 in HepG2 and HepG2.2.15 three hours after CPT treatment (left). The percentage of positive

cells was quantified against DAPI staining (right). n = 3 experimental repeats. Scale bar: 50 microns. Error bars: s.d. * = $p<0.05$; ** = $p<0.01$. (B) Immunoblotting for phosphorylated RPA32 (pSerine 4/8) in HepG2 and HepG2.2.15 cells. (C) Illustration for mechanism of DNA end resection. Upon DNA damage, MRE11/RAD50/NBS1 (MRN) and CtIP process DNA ends and generate a short stretch of ssDNA that is coated by RPA (green). Subsequently, EXO1 and BLM-DNA2 nucleases carry out processive nucleolysis to generate long-range RPA-coated ssDNA. RAD51 then replaces RPA and initiate HR. (D) Quantification for RAD51 and RPA32 IRIF as in Fig.1D. (E) Secreted HBsAg and HBeAg assessed by ELISA for HBV-infected PHH culture on indicated days. PHHs were infected with concentrated supernatants of HepG2.2.15 culture. (F) PHHs were pre-incubated with concentrated supernatants of HepG2.2.15 cells or a patient serum with high titre of HBV. Percentage of infection was quantified by indirect immunofluorescence for HBcAg (green) at day 7.

Ren L, et al. Fig. S2

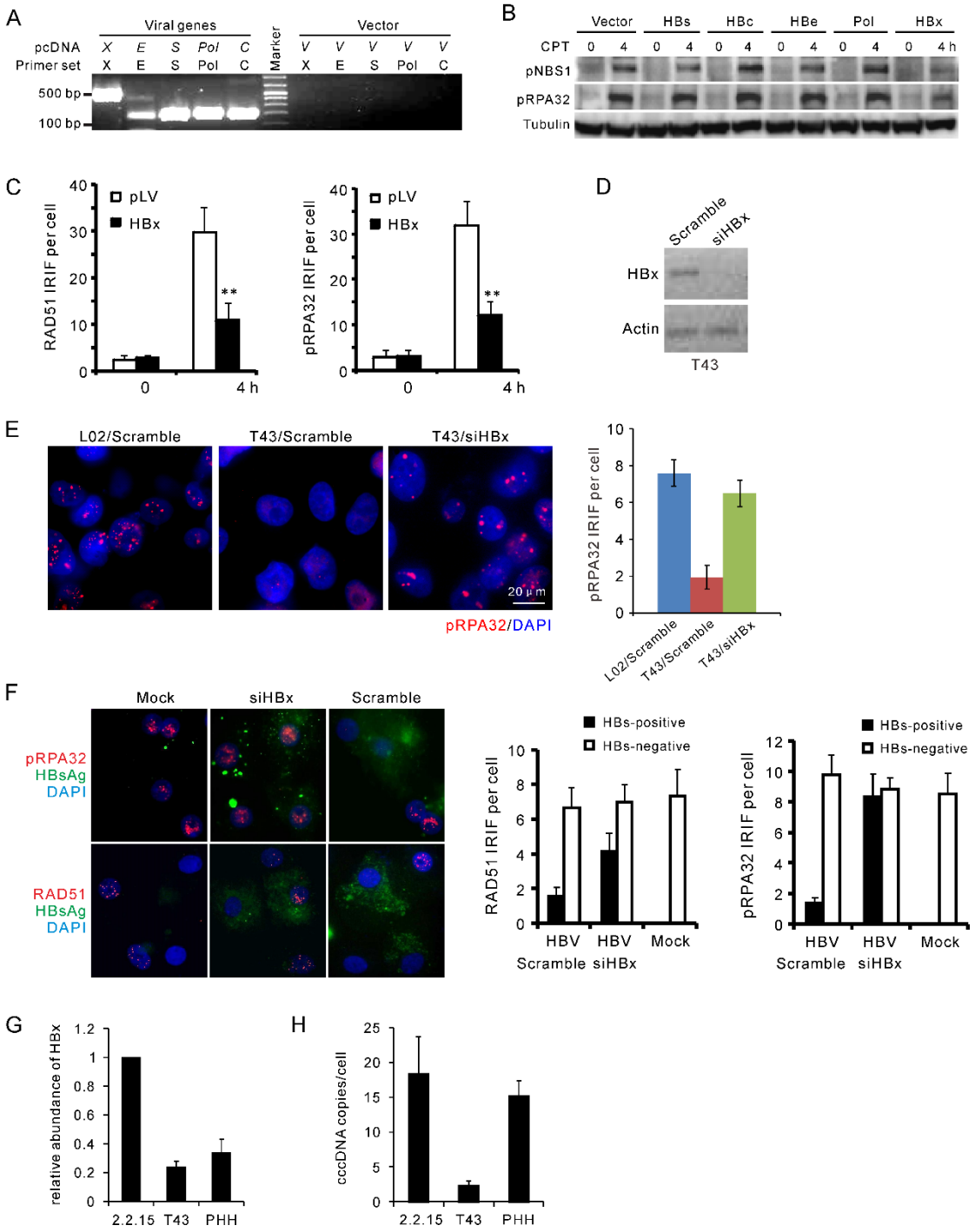

Fig.S2 (A) Detection of mRNA of indicated viral genes expressed from pcDNA3 vector in L02 cells. X: *HBx*, E: *HBe*, S: *HBs*, *POL*: HBV viral polymerase, C: *HBc*. (B) Screen for HBV-encoded viral genes implicated in resection interference by immunoblotting. Phosphorylated RPA32 (pSerine 33) and NBS1 (pSerine 343) were used as markers for DNA damage. (C) Quantification of RAD51 and pRPA32 foci for experiments in Fig. 2B. (D) Semi-quantitative RT-PCR for *HBx* in T43 cells pre-treated with *siHBx* or not.

Messenger RNA of Actin was quantified as internal control. (E) Representative image and quantification for pRPA32 foci in T43 cells with or without *siHBx* treatment. IRIF was monitored 4 hours after 1 Gy irradiation. (F) Representative images (left) and quantification (right) of pRPA32 and RAD51 IRIF in HBV infected PHHs with treatment of siHBx or not. IRIF was counted in HBsAg-positive or negative cells in parallel. (G-H) Determination of relative abundance of *HBx* mRNA by RT-qPCR (G) and cccDNA copy number per cell by real-time PCR (H). PHHs infected by HBV were collected for experiments 7 days after inoculation.

Ren L, et al. Fig. S3

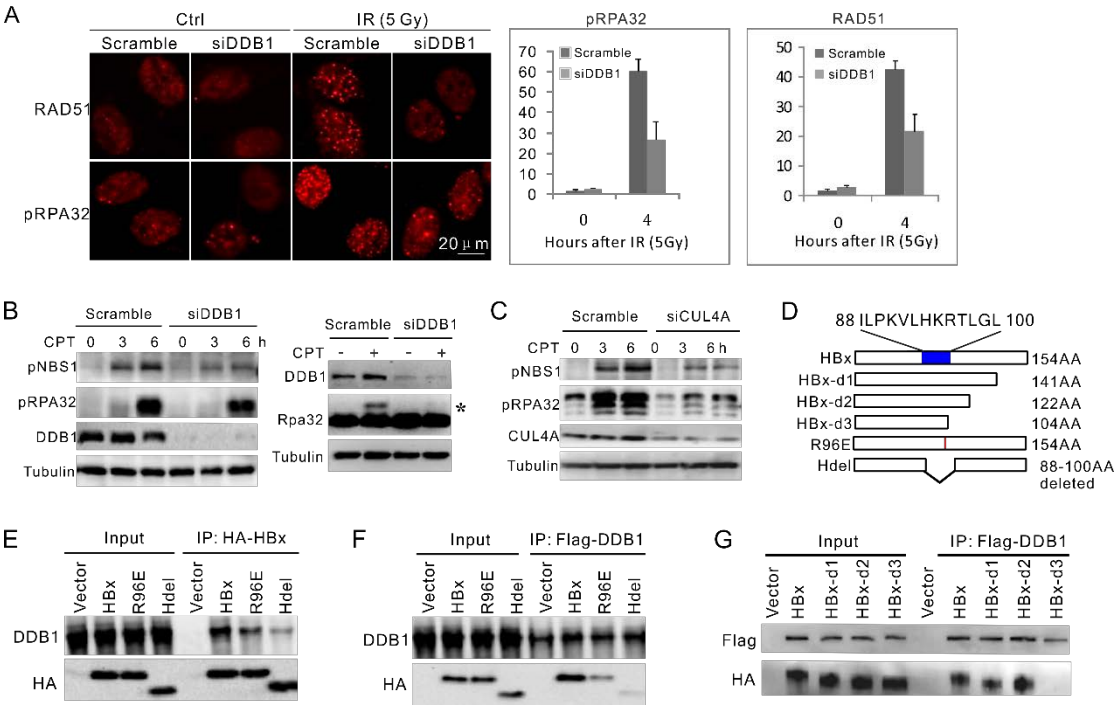

Fig.S3 Impact of HBx on CRL4-dependent DNA end resection through its H-box motif. (A) Indirect immunofluorescence (left) and quantification (right panels) for indicated IRIF in 293T cells 4 hours post-IR. pRPA32: phosphorylated Serine 33. (B-D) Immunoblotting for CPT-induced RPA32 and NBS1 phosphorylation in L02 cells pre transfected with DDB1 (B) or CUL4A (C) siRNA. RPA32 was probed with anti-rabbit serum or anti-pSerine 33 of RPA32. Asterisk: phosphorylated form of RPA32 detected by anti-serum. (D) Schematic representation for HBx point and deletion mutants. Hdel: HBx with deleted H-box (residuals 88-98). Blue bar: H-box, red line: Arg96Glu. (E) Immunoprecipitation assays performed in L02 cells using the indicated H-box mutants of HA-tagged HBx to pull down endogenous DDB1. Vector: empty pcDNA3-HA plasmid. Five percent of input material was analyzed as control. (F) Indicated alleles of HA-HBx were pulled down by Flag-DDB1 using anti-Flag antibody. All samples were transfected with pcDNA3-Flag-DDB1 whose expression was probed by Rabbit anti-DDB1. Vector: empty pcDNA3-HA plasmid. (G) Pull-down of HA-tagged C-terminal deletion mutants of HBx by Flag-DDB1 from 1 mg of L02 cell extracts. Vector: empty pcDNA3 plasmid.

Ren L, et al. Fig. S4

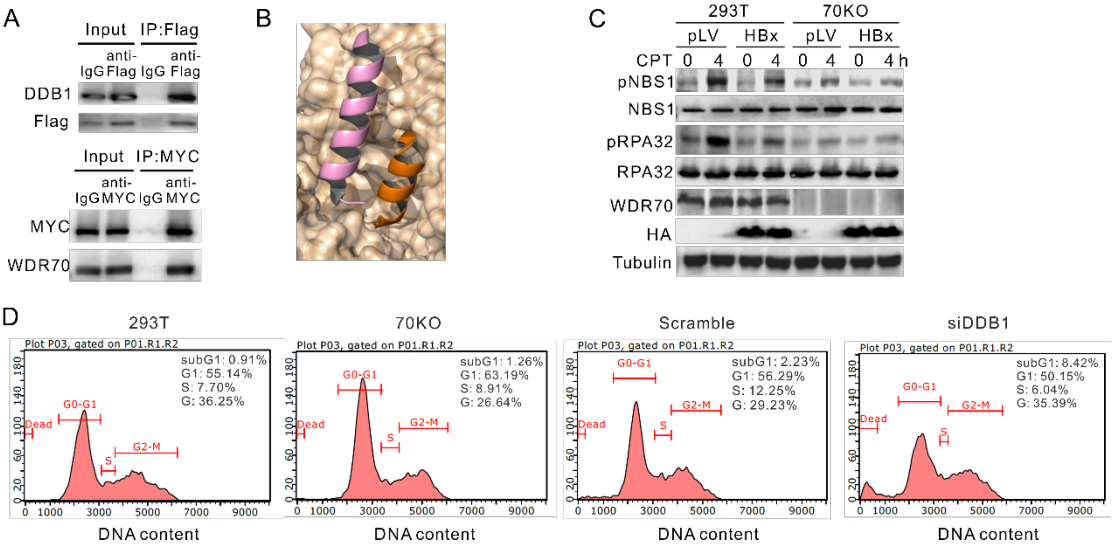

Fig.S4 HBX interferes with resection by disrupting the complex integrity of $CRL4^{WDR70}$. (A) IP analysis from 1 milligram of L02 soluble extracts using Flag-WDR70 or Myc-DDB1 to precipitate endogenous interacting proteins. IgG was used as negative controls. (B) Illustration of H-box (brown) and α-helix (pink) from DDB2 as shown in previous figure. H-box is believed to be the core structural element of DDB2 for interacting with DDB1, the adjunct long α-helix forms a large contact surface on the shallow concave on DDB1. Structurally, the α-helix folds on the top of H-box and provides extra binding capabilities between DDB2 and DDB1. WDR70 is predicted likely to interact with DDB1 by the identical mode. (C) Immunoblotting for phosphorylated RPA32/NBS1 in parental and *WDR70* knockout 293T cells with or without HBx expression. Phosphorylation defects in *WDR70*-depleted cells were not exacerbated by introducing HBx. (D) FACS analysis showing the cell cycle profiles of $WDR70^{KO}$ (70KO) and *siDDB1* cells. Loss of these genes resulted in relatively minor decrease of S/G2 populations considering the marked inhibition of resection.

Ren L, et al. Fig. S5

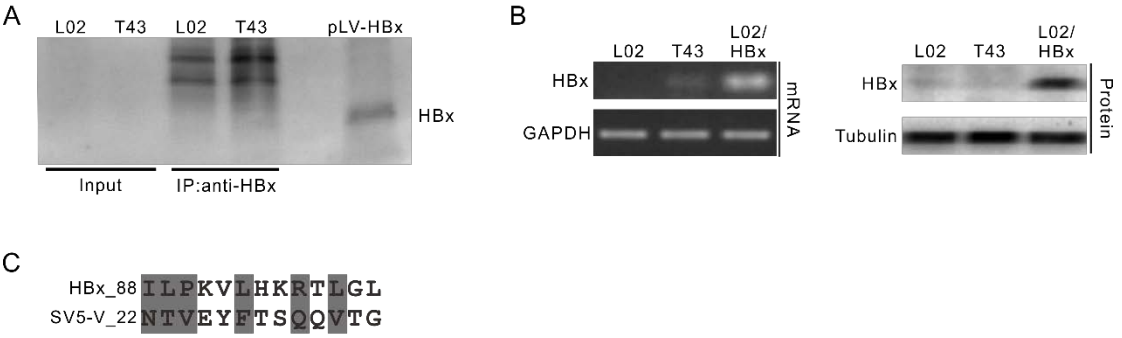

Fig.S5 (A) Immunoblotting for HBx enriched by immunoprecipitation of T43 cell lysates. No HBx protein was effectively detected in T43 due to low expression level and limit of sensitivity rabbit α-HBx antibody. However, HBx could be monitored in total lysate of L02 cells infected by Lenti-HBx. (B) Comparison for mRNA (upper panel) and protein (lower panel) levels for *HBx* expressed from lentivirus (L02/HBx) or integrated HBV genomes in T43 cells. Note that HBx protein was not monitored in T43 but was detectable in HBx-expressing L02 cells. (C) Homology alignment of H-box between SV5-V (residuals 22-34) and HBx (residuals 88-100).

Ren L, et al. Fig. S6

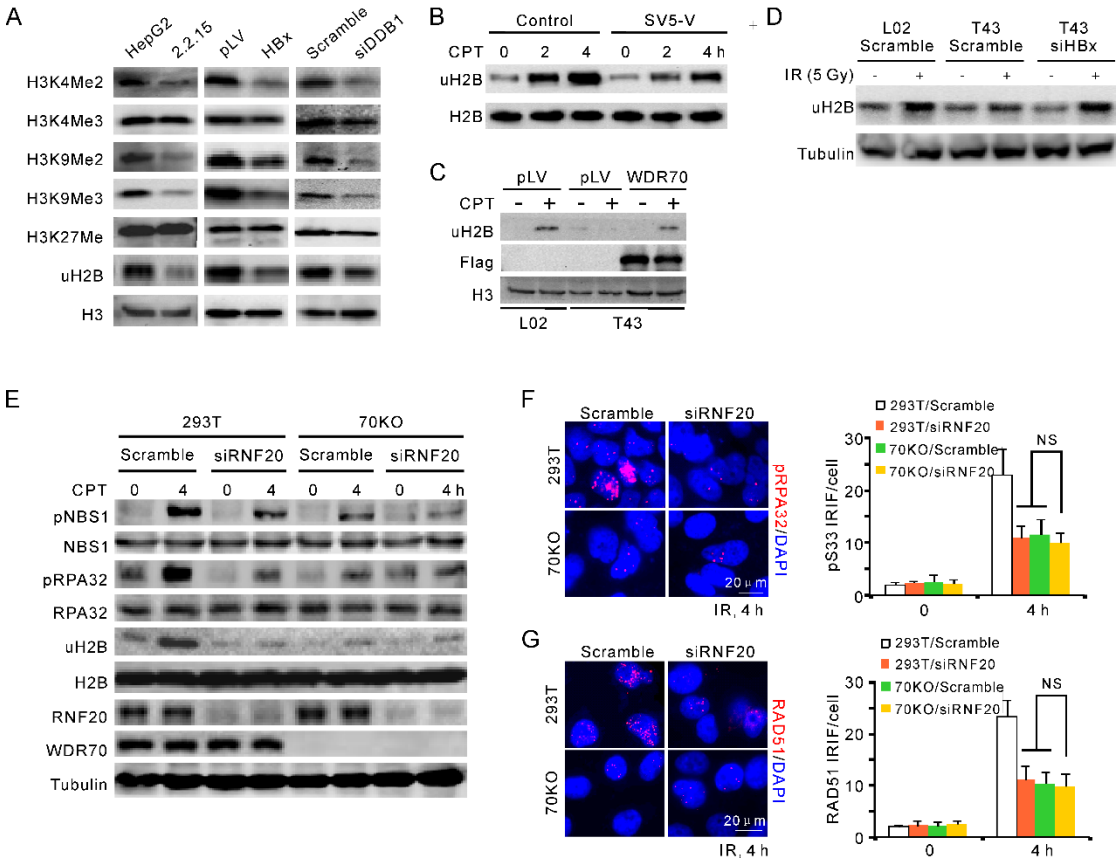

Fig.S6 Impact of HBx on WDR70 and HULC^{RNF20}-dependent H2B monoubiquitination. (A) Screen for altered histone modifications by immunoblotting the whole cell lysates from HepaG2.2.15, or *HBx*-expressing and si*DDB1* L02 cells. Apart from impaired H2B monoubiquitination, there were notable decrease of di-methylation of H3K4, di- and tri-methylation of H3K9, which reflect disturbed trans-histone regulation resulting from reduced uH2B. (B) Detection of CPT-induced uH2B in L02 cells transfected with *SV5-V* or empty plasmids. (C) Same as Figure 5F, expression of Flag-WDR70 restored H2B monoubiquitination levels by in T43 cells. Cells were treated by 2 uM CPT for 2 hours. (D) Western blotting for uH2B in L02 or T43 cells treated with scramble siRNA or *siHBx*. (E) Immunoblotting for pNBS1/pRPA32 (pSerine 33) and H2B monoubiquitination upon CPT treatment in *WDR70*^{KO} (*70KO*) and 293T cells transfected with indicated siRNA. α-RPA32 and α-NBS1 probed for de-phosphorylated proteins treated by CIP phosphotase. (F, G) Foci analysis for pRPA32 (F) and RAD51 (G) showing the epistasis of *RNF20* and *WDR70* in resection and HR. n = 3 biological repeats. Error bars = s.d. NS: no significant difference.

Ren L, et al. Fig. S7

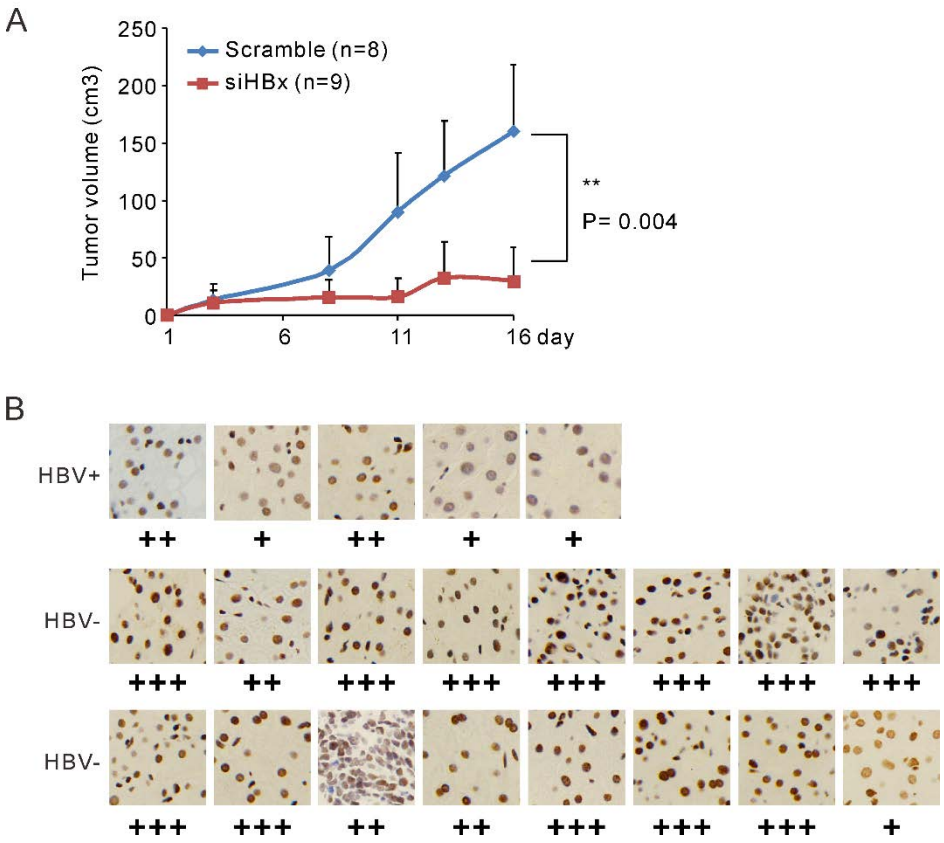

Fig.S7 (A) Xenograft tumor formation assay of T43 cells in nude mice. Indicated double stranded siRNA was injected with *in vivo* RNA transfection reagent (Biotool) via tail vein. Individual tumor volumes were measured at 2-4 days intervals. Error bars: s.d.. (B) Representative uH2B staining of non-cancerous human liver tissue with same IHC method as in Fig. 8A.

Ren L, et al. Fig. S8

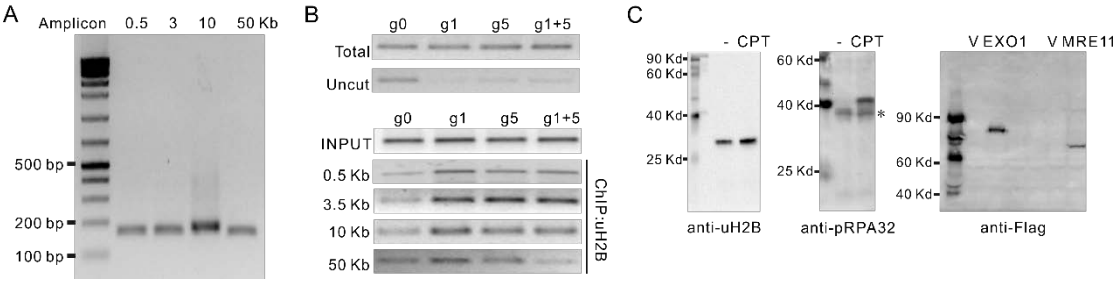

Fig.S8 (A) Test of specificity of PCR amplifications used in CRISPR-DSB system described in Fig.6. PCR fragments were run through 2% agarose gels. (B) Analysis for the efficiency of gRNA (g1 and g5)-directed DSB induction and uH2B enrichment at *PPP1R12C/p84* locus of 293T cells 24 hours after transfection. Upper panel: Induction of DSBs was indicated by the disappearance of Uncut DNA (primers 55/56 across targeting sequence). Total DNA (primers 53/54) was amplified as internal control of input genomic DNA. Lower panel: Ubiquityl modification of H2B at indicated distances from the DSB was monitored by semi-quantitative PCR after chromatin IP. g0: empty vector encoding no gRNA serves as a negative control. (C) Immunoblotting verifying the antibody specificity applied in ChIP analysis. Exo1 and Mre11 were Flag-tagged. *: basal level of pRPA32 without CPT challenge. V: empty Flag-tag vector.

Supplemental Methods

Cell lines and Plasmids

L02, T43 (derived from L02), HEK293T and their derived cell lines were cultured in DMEM supplemented with 10% FBS, whereas HepG2 and HepG2.2.15 were maintained in RPMI 1640. PHHs (Bioreclamation IVT) were maintained in INVITROGRO HI Medium (Bioreclamation IVT, Z990012).

For cloning of individual HBV viral genes, PCR fragments of each gene were amplified from an HBV-genome plasmid and inserted into the *Eco*RI / *Xho*I sites of pcDNA3. Lentiviral vectors for expressing *HBx* and *DDB1* were created by inserting individual PCR fragments into the *Xba*I site of pLVX-IRES-ZsGreen/Puro using the In-Fusion cloning kit (Clontech, 639650). Human *WDR70* and *USP22* expressing plasmids were created by inserting the relevant ORF into the *Eco*RI site of pLVX-IRES-ZsGreen. The pcDNA3-HA-HBx full length and C-terminal truncations (consisting of residues1-141, 1-122, and 1-104) were created by inserting individual PCR fragments into the *Eco*RI site of pcDNA3-HA. The *R96E* hypomorph of *HBx* was generated with a QuikChange site-directed mutagenesis kit (Stratagene, 200518) using primers 7/8 (AGG to GAG at 286-288 bp). All plasmids used in this study are listed in Tables S1 and S2.

Establishment of knockdown, knockout and overexpression cells

Stable knockdown or overexpression of target genes was achieved using a lenti-viral based delivery system or plasmid transfection. Transfections were carried out using Lipofectamine 2000 (Invitrogen, San Diego, CA) or X-tremeGENE HP (Roche, 06366244001). *WDR70* knockout in 293T was accomplished following the gRNA provider's protocol (1). Single duplex siRNA employed in this study were purchase from Ribobio (Guangzhou, China). The details of RNA interference, Lentivirus packaging and infection are described in the next two paragraphs.

RNA interference

All siRNAs employed in this study were single duplex siRNA purchase from Ribobio (Guangzhou, China). Individual siRNA duplexes used were: *DDB1* (siB09531141904, target sequence: 5'-CCUGUUGAUUGCCAAAAAC-3' or siG1098103838, 5'-CUCCUUGGAGAGACCUCUA-3'), *WDR70* (siG1117130927, target sequence: 5'-CUGCCAGAAUGGAAGCAUA-3'), *RNF20* (target sequence: 5'-CCAATGAAATCAAGTCTAA-3') and HBx (siB181219052640, target sequence: 5'-CTAGGAGGCTGTAGGCATA-3'). RNAi transfections were performed using

Lipofectamine 2000 or X-tremeGENE siRNA Transfection Reagent (Roche, 04476093001) following manufacturer's instruction. Normally, two consecutive rounds of siRNAs transfections were carried out and cells were assayed 48 hours after second round. Lentiviral vectors encoding shRNA GV112-shWDR70 (target sequence: CTGCCAGAATGGAAGCATA)) were purchased from GeneChem, and packaged into lentiviral particles following the method described above. To knockdown *HBx* expression in xenografted T43 cells (Supporting Fig. S7A), *in vivo* RNA knockdown in mice was performed by injecting siRNA (50 ug) and 25 ul RNA transfection reagent (Biotool, B45215) via tail vein.

Lentivirus packaging and infection

For packaging of lentivirus encoding protein or shRNA (see Table 1), 5 x 10^6 of 293T cells was co-transfected with package system (pLVX-IRES-ZsGreen/Puro, pMD.2G and psPAX2) using X-tremeGENE HP DNA Transfection Reagent. Medium containing secreted virion was collected 72 hours after transfection and stored at minus 80^{o}C. Infectivity of supernatant was determined by positive clones (GFP or puromycin-resistant) in 96 well plates at 10-fold serial dilution. 293T, L02 or T43 cells were infected at a titre of 2 MOI/cell unless stated otherwise. Cells with stably integrated lentivirus were propagated in DMEM supplemented with 10% FBS up to one month for experimental use.

HBV virion preparation and infection

Preparation of HBV virions for PHH infection were performed using Ni and Schulze's methods (2, 3) with minor modifications. Briefly, HBV virions used in infection assays were either concentrated with 6% PEG8000 from supernatants of HepG2.2.15 cell culture or from patient sera with high titers of HBV (4×10^9 copies/ml). Cryopreserved PHHs were thawed and seeded in plating medium (Bioreclamation IVT, Z99029) on collagen-coated plates, replaced by incubating medium (Bioreclamation IVT, Z990012) supplemented with 1.5% DMSO 8 hours later. After 24 hours, PHHs cells were infected with a MOI (multiplicity of infection) of 1000 viral genome equivalents (VGE) in the presence of 4% PEG8000 and 1.5% DMSO. Infectivity was determined by monitoring HBV antigens with ELISA for HBsAg/HBeAg or immunostaining for HBcAg.

HBV cccDNA and HBx mRNA analyses

Real-time PCR quantification of HBV cccDNA were performed in triplicate according to the manufacturer's instructions (Jianglai Biotech Company, Shanghai, China). HBV

cccDNA copy numbers were calculated with a standard curve from positive control samples with known nucleic acid quantities.

Total RNA was extracted (OMEGA, R6934-01) with extended DNase digestion to remove contaminated HBV DNA and used for reverse-transcription of cDNA using random primers and GoScript reverse transcriptase (Promega, A5001). Real-time PCR for HBx (5'-TTCACCTCTGCACGTCGCATGGAG-3' (forward) and 5'-CCTACAGCCTCCTAGTACAAAGACCT-3' (reverse) was carried out with SYBR Premix Ex Taq (Promega, A6002) on Stratagene Mx3000P Real-Time PCR System. Relative expression of HBx was calculated according to the $2^{\wedge-\triangle\triangle CT}$ method, normalized to human GAPDH gene.

Measurement of DNA damage responses

DSBs were induced by irradiating cells at 1 Gy/min using a custom-made X-ray machine (Wandong Ltd, Beijing). Unless stated otherwise, CPT treatment was carried out at 2 μM for the indicated time. Cells after genotoxic challenge were either fixed with 4% paraformaldehyde (PFA) or lysed in Lamilli SDS sample buffer for IF or immunoblotting, respectively.

Immunofluorescence and microscopy

Cells grown on glass coverslips were fixed with 4% PFA, followed by permeabilization in PBS containing 0.3% TritonX-100. After blocking in 5% BSA/0.1% Tween-20 PBS for 30 min, cells were incubated with diluted primary antibody (Table 3) and subsequently labelled with secondary antibodies (α-mouse-FITC or α-rabbit-Cy3) for 30 min at 37°C. Following three washes with PBS, cover slips were mounted with anti-fade medium containing 4,6-diamidino-2-pheny-lindole (DAPI). Images were obtained using Olympus fluorescence microscope (BX51).

For native BrdU detection, exponentially growing cells were pulsed with 1 μM BrdU for 48 hours (4), challenged by 2 μM CPT and recovered for 4 hours. Cells were fixed in methanol at -20°C for 20 minutes and blocked in 5% BSA in PBS for 30 minutes, followed by standard IF procedure. For visualization of the genomic incorporation of BrdU in parallel samples, DNA was denatured by 0.4N HCl for 25 min after fixation, and standard protocol of permeabilization and antibody incubation were carried out. All quantitative immunofluorescent analysis was performed by counting 100-200 cells from 3 independent experiments.

Immunoblotting

To prepare total cell extracts, cells were directly lysed and boiled in an SDS sample buffer (50 mM Tris–HCl [pH 6.8], 1% SDS, 10% glycerol, 5% mercaptoethanol, 0.01 % bromophenol blue). Cell lysates were then resolved by SDS-PAGE and transferred to PVDF membrane (Roche, 03010040001), followed by antibody incubation in 5% BSA/TBST Buffer (50 mM Tris, 150 mM NaCl, 0.1% Tween 20, [pH 7.6]). Chemiluminescent visualization was performed with horseradish peroxidase-conjugated goat α-rabbit IgG (DAKO, P0448) or rabbit α-mouse IgG (DAKO, P0260), and detected using ChemiDoc XRS system (Bio-Rad). To compare the total protein levels of RPA32 from different cells and treatments, whole cell extracts were de-phosphorylated by 10 units of Alkaline Phosphatase at 37°C for 30 min before immunoblotting. Abbreviations for antibodies: pS33: RPA32 (pSerine 33); pNBS1: NBS1 (pSerine 343). Antibodies used in this study were listed in Table S3. Relative band densitometry in Figure 5 was determined by NIH-ImageJ.

Immunoprecipitation

co-Immunoprecipitation was conducted to investigate the physical interaction between DDB1, WDR70 and HBx. Briefly, 4×10^6 cells were lysed on ice in Nonidet P-40 Lysis Buffer (50 mM Tris-HCl [pH 8.0], 100 mM NaCl, 5 mM $MgCl_2$, 1% NP-40, supplemented with protease inhibitor cocktail) for 40 min and cell extracts were cleared by centrifugation at 13,000×*g* for 10 min at 4°C. Supernatants were incubated for 2 hours with 4 μg of appropriate antibodies at 4°C followed by 1-hour absorption with Protein G DynaBeads (Invitrogen, 10004D). α-Flag M2 magnetic beads (Sigma, M8823) were applied to pull down Flag-tagged immunocomplex. Precipitated protein complexes were washed four times with Lysis Buffer and boiled in SDS sample buffer followed by SDS-PAGE and immunoblotting. For co-IP of DDB1 and HBx mutants, cell lysates were prepared 72 hours after transfecting Flag-DDB1 or HA-HBx plasmids into L02 cells. To analyse DDB1-WDR70 interaction in L02 and T43 cells, cell lysates were extracted 48 hours after infection with WDR70-Flag or empty lentivirus. Low-titre (0.2 MOI) of viruses was applied to avoid over-competition of WDR70 against low level of HBx, where only ~20% of the cells were infected as determined by GFP signal co-translated with WDR70 through IRES.

Cell cycle analysis

Cells were harvested by trypsinization and fixed with ethanol (70%). After washed with PBS, Cells were resuspended in a 50 μg/ml of propidium iodide (PI) in PBS, and flow cytometry was performed to monitor cell cycle. For FUCCI analysis of RPA and

RAD51 IRIF in S/G2 cells, reporter plasmids encoding fluorescent mAG-hGeminin were transfected into cells, followed by treatment with IR 48 h after transfection. Cells were fixed 4 hours post-IR and subjected to immunofluorescent analysis.

Chromatin fractionation

Cells were lysed in buffer A (10mM HEPES [pH 7.9], 10 mM KCl, 1.5 mM $MgCl_2$, 0.34 M sucrose, 10% glycerol, 0.1% Triton X-100, supplemented with protease inhibitor cocktail) for 5 min on ice. Cytosolic and nuclei fractions were separated by centrifugation at 1300×g for 4 minutes at 4^{o}C (5). Nuclei were washed once in buffer A, and lysed in buffer B (3 mM EDTA, 0.2 mM EGTA, 1 mM DTT, supplemented with protease inhibitor cocktail), followed by centrifugation for 1700×g at 4°C for 4 minutes. The chromatin pellet (insoluble chromatin) were washed once in buffer B and directly lysed and boiled in an SDS sample buffer.

CRISPR-induced chromosomal DSB

To generate CRISPR-gRNA-directed DSB at Intron 1 of the *PPP1R12C/p84* locus, the CRISPR-gRNA vector (pMC1-1-p84-g1, targeting sequence: 5'-GTCCCCTCCACCCCACAGTGGGG-3' and pMC1-1-p84-g5, targeting sequence: 5'- AGAACCAGAGCCACATTAACCGG -3') was transfected in 293T or *WDR70* knockout cells for 24 hours before genomic DNA extraction or ChIP assay. The CRISPR-gRNA backbone plasmid (g0) expressing no gRNA sequence was used as the negative control. Cells were pre-infected by 2MOI of lentivirus (HBx or 2KR) 24 hours before gRNA introduction to evaluate the effects of HBx on DSB responses. To evaluate the cutting efficiency of the CRISPR-RNA complex, genomic DNA from 20,000 cells was directly amplified by Terra PCR Direct Polymerase Mix (Clontech, ST0288) followed by proteinase K treatment at 37^{o}C for 30 min. Disappearance of the amplicon (Primers 55/56) spanning >100 bp beyond both 5' and 3' direction of the targeting sequence indicates the induction of DSB at the *PPP1R12C/p84* locus (Supporting Fig. 7B). Total DNA (amplicon 50 Kb, primers 53/54) was used as internal control.

Chromatin immunoprecipitation (ChIP)

ChIP assays were performed as previously described with minor modifications (6). Briefly, for each location analysis, approximately 4×10^6 cells were harvested followed by 10 min cross-linking with formaldehyde at a final concentration of 1% and washed twice in PBS. They were lysed in Lysis Buffer (50 mM HEPES [pH7.4], 140 mM NaCl, 1% Triton X-100, 0.1% NaDeoxycholate, 1 mM EDTA supplemented with protease

inhibitor cocktail (Roche, 11836170001)), sonicated to solubilise chromatin and shear the cross-linked DNA. Sonication were performed at 4ºC with JY92-2II DN (XinYi, Ning Bo, China) at power of 600 Watt for 10×115 second pulse (3 second pause between pulses). To retrieve chromatin-associated proteins, the whole cell extracts were incubated on a rotator overnight at 4ºC with 10 µl magnetic Protein G Dynabeads (Invitrogen, 10004D) pre-coated with 2 µg indicated antibodies and 100 µg sperm DNA. The beads were washed five times with Lysis Buffer, Lysis High Salt Buffer (50 mM HEPES [pH7.4], 500 mM NaCl, 1% Triton X-100, 0.1% NaDeoxycholate, 1 mM EDTA), Wash Buffer (10 mM Tris [pH8.0], 250 mM LiCl, 0.5% NP40, 0.5% NaDeoxycholate, 1 mM EDTA) and TE buffer [pH8.0] for two times, respectively. Bound DNA-Immune-complexes was eluted off the beads in elution buffer (50 mM Tris [pH8.0], 1% SDS, 10 mM EDTA) by heating at 65ºC for 2 hours. DNA was purified using a Gel Extraction Kit (Omega, D2500-02). Whole cell extracts were treated parallelly for cross-link reversal and DNA extraction. 200ng recovered DNA was used for each PCR reaction using Platinum® *Taq* DNA Polymerase (Invitrogen, 10966). All reactions were performed in triplicate and repeat for three times. Primer sets used to measure protein enrichment: 0.5 kb, pair 47/48; 3.5 kb, pair 49/50; 10 kb, pair 51/52; 50 kb, pair 53/54. Primers 51/52 were used to amplify input DNA as internal control. Specificities for primers and antibodies used in ChIP assays were tested in Supporting Fig.S8A-C.

Xenograft experiments

For anti-tumour analysis using xenograft animal models, female athymic nude mice (BALB/cSLC-nu/nu, SPF) starting at 4 weeks of age were used for all the experiments. We used the binomial distribution to calculate sample sizes. To assess the tumorigenecity of L02 or T43 cells *in vivo*, mice were subcutaneously inoculated in both sides of armpits or hind flanks (2×10^6 cells *per* site). Inoculated mice were observed daily over the period until termination of the experiments. Moribund mice or mice with obvious tumours were killed and subjected to necropsy and IHC inspection. Individual tumors were weighted after dissection. For excluding outliers of tumour volume, Grubbs' test was applied (Gi>GO. 95, two-tailed test).

Immunohistochemistry and Dual-rated semi-quantitative IRS analysis

Immunohistochemistry follows standard methods of fixation and staining. Briefly, deparaffinized tissue sections were treated with graded alcohol series. Following antigen unmasking with citrate-based solution, endogenous peroxidase activity was

quenched by immersing tissue sections in H_2O_2/methanol solution and protein blocking reagent. Slides were incubated with mouse α-uH2B and visualised by Avidin-Biotin complex (ABC)-diaminobenzidine (DAB) staining kit (Vector laboratory). Nuclei were counterstained with hematoxylin. All immunostained slides were examined by a pathologist blinded to the clinical outcome. For scoring of the uH2B positivity from clinical HCC, an immunoreactivity score (IRS) was calculated as the product of staining intensity (SI) multiplied by percentage of positively stained cells (PP) (7). SI was defined as a four-point gradient scale (0: no staining; 1: weak/light yellow; 2: moderate/bright yellow; 3: strong/brown). PP was defined according to a four-point positive-negative scale (0: 0-9% positive cells; 1: 10%-25% positive cells; 2: 26%-50% positive cells; 3: 51%-75% positive cells; 4: >75% positive cells). Statistic significance (mean/±SD) was analysed by Graphpad Prism and two-tail *t*-test.

Study approval

All mice were maintained and handled according to protocols approved by the Animal Care and Ethics Committee of Sichuan University. For experiments involving human materials (Table S4), all performance of sample request, collection and processing were informed and consented by patients in written forms, and were carried out in accordance with the Ethics Guidelines and Regulation of individual academic institutes. This study was approved by the Ethics Committee of Shanxi Medical University and Sichuan University.

Reference for Supplemental Materials

1. Zeng M, Ren L, Mizuno K, Nestoras K, Wang H, Tang Z, Guo L, et al. CRL4(Wdr70) regulates H2B monoubiquitination and facilitates Exo1-dependent resection. Nat Commun 2016;7.
2. Ni Y, Urban S. Hepatitis B Virus Infection of HepaRG Cells, HepaRG-hNTCP Cells, and Primary Human Hepatocytes. Methods Mol. Biol. 2017;1540:15-25.
3. **Schulze A, Mills K**, Weiss TS, Urban S. Hepatocyte polarization is essential for the productive entry of the hepatitis B virus. Hepatology 2012;55:373-383.
4. **Bunting SF, Callen E**, Kozak ML, Kim JM, Wong N, Lopez-Contreras AJ, Ludwig T, et al. BRCA1 functions independently of homologous recombination in DNA interstrand crosslink repair. Mol Cell 2012;46:125-135.
5. Mendez J, Stillman B. Chromatin association of human origin recognition complex, cdc6, and minichromosome maintenance proteins during the cell cycle:

assembly of prereplication complexes in late mitosis. Mol Cell Biol 2000;20:8602-8612.

6. **Mathur D, Danford TW**, Boyer LA, Young RA, Gifford DK, Jaenisch R. Analysis of the mouse embryonic stem cell regulatory networks obtained by ChIP-chip and ChIP-PET. Genome Biol 2008;9:R126.
7. Li JC, Yang XR, Sun HX, Xu Y, Zhou J, Qiu SJ, Ke AW, et al. Up-regulation of Kruppel-like factor 8 promotes tumor invasion and indicates poor prognosis for hepatocellular carcinoma. Gastroenterology 2010;139:2146-2157.

Table S1. Plasmids used in this study

Plasmids	Source
pcDNA3-HBV	Gift from Dr Huaidong Hu, Chong Qing Medical University
pcDNA3-HA-HBx	This study
pcDNA3-HA-HBx-R96E	This study
pcDNA3-HA-HBx-d1	This study
pcDNA3-HA-HBx-d2	This study
pcDNA3-HA-HBx-d3	This study
pcDNA3-HA-HBx-Hdel	This study
pCMV-Flag-WDR70	This study
pgRNA-WDR70	gRNA vector for *WDR70* knockout, Purchased from ViewSolid Biotech
pCDH-Cas9	Purchased from ViewSolid Biotech
pLVX-Green	Purchased from Clontech632187
pLVX-G-WDR70-Flag	This study
pLVX-G-WDR70-Flag -Hbox-del	This study
pLVX-G-Flag-DDB1	This study
pLVX-G-HBx	This study
pLVX-puro-HA-HBx	This study
pLVX-puro-HA-HBx-Hdel	This study
pcDNA3-Myc-DDB1	This study
pLVX-G-H2B	This study
pLVX-G-2KR	This study
pLVX-G-shWDR70	Purchased from Genechem
pLVX-G-Flag-RNF20	This study
pcDNA3-HBsAg	This study
pcDNA3-HA-HBcAg	This study
pcDNA3-HA-Polymerase	This study
pcDNA3-HA-HBeAg	This study

pMC1-1-p84-g1	gRNA vector for *PPP1R12C/p84* locus, Purchased from Viewsolid biotech
pMC1-1-p84-g5	gRNA vector for *PPP1R12C/p84* locus, Purchased from Viewsolid biotech
pMC1-1-p84-g0	gRNA vector (empty), Purchased from Viewsolid biotech

Table S2. Primers used in this study

	Primers	Application
Primer 1	GGATCTATTTCCGGTGAATTCAAATTAGCC GGCACCTGTAATCCC	gRNA^{WDR70}-F
Primer 2	AGAACTAGTCTCGAGGAATTCGTTGGTTCC AACGGATAACGCAGA	gRNA^{WDR70}-R
Primer 3	AAATTAGCCGGCACCTGTAATCCC	WDR70 Exon 1 sequencing, forward
Primer 4	GTTGGTTCCAACGGATAACGCAGA	WDR70 Exon 1 sequencing, reverse
Primer 5	CAAA GAA TTCATGGCTGCTCGGTTGTGCT	HBx to pcDNA3-HA, forward
Primer 6	CCAAGGGCCCGGCAGAGGTGAAAAAGTTG C	HBx to pcDNA3-HA, reverse
Primer 7	ACAGTCTTACATAAGGAGACTCTTGGACTC TCAGGA	HBx R96E mutagenesis, Forward
Primer 8	TCCTGAGAGTCCAAGAGTCTCCTTATGTAA GACTGT	HBx R96E mutagenesis, reverse
Primer 9	CGTTGACATTGCAGATCGGTGGGCGTTCAC GGTGG	HBx H-box deletion, forward
Primer 10	TCTGCAATGTCAACGACCGA	HBx H-box deletion, reverse
Primer 11	TTCCTCGAGACTAGTTCTAGAGCCACCATG GCTGCTCGGTTGTGCTG	HBx to pLVX-G, forward
Primer 12	GGGATCCGCGGCCGCTCTAGATTAGGCAGA GGTGAAAAAGT	HBx to pLVX-G, reverse
Primer 13	GCGGTCGGCGCGGGAGGATCCATGTACCCA TACGATGTTCCAGATTACGCTGCTGCTCGGT TGTGCT	HA-HBx to pLVX-puro, forward
Primer 14	GGAGGGAGAGGGGCGTTAGGCAGAGGTGA AAAAG	HA-HBx to pLVX-puro, reverse
Primer 15	GGATCTATTTCCGGTGAATTCGCCACCATG GAGCGCTCTGGGCCCAG	WDR70-Flag to pLVX-G, forward

Primer 16	AGAACTAGTCTCGAGGAATTCTCACTTATC GTCGTCATCCTTGTAATCAATTTTACGTTTT TTCC	WDR70-Flag to pLVX-G, reverse
Primer 17	CCGAGGATTACTGTCATCGG	WDR70-Hdel-Flag to pLVX-G, forward
Primer 18	GACAGTAATCCTCGGGAAGACAGCCCATAT TGGGT	WDR70-Hdel-Flag to pLVX-G, reverse
Primer 19	ATGGAGGCCCGAATTATGTCGTACAACTAC GTGGT	DDB1 to pcDNA3-Myc, forward
Primer 20	ACCTCGAGCCGAATTCTAATGGATCCGAGT TAGCT	DDB1 to pcDNA3-Myc, reverse
Primer 21	TTCCTCGAGACTAGTTCTAGAGCCACCATG GATTACAAGGATGACGACGATAAGTCGTAC AACTACGTGGT	Flag-DDB1 to pLVX-G, forward
Primer 22	GGGATCCGCGGCCGCTCTAGACTAATGGAT CCGAGTTAGCT	Flag-DDB1 to pLVX-G, reverse
Primer 23	TTCCTCGAGACTAGTTCTAGAGCCACCATG CCCGAGCCCTCA AAG	H2B to pLVX-G, forward
Primer 24	GGGATCCGCGGCCGCTCTAGA TCACTTGGAACTGGTGTACTTGGT	H2B to pLVX-G, reverse
Primer 25	GGGATCCGCGGCCGCTCTAGA TCACCTGGAACTGGTGTACCTGGT	2KR to pLVX-G, reverse
Primer 26	ATAAAGAATTTGGAGCTACTG	HBc RT-PCR, forward
Primer 27	CAGGTAGCTAGAGTCATTAGT	HBc RT-PCR, reverse
Primer 28	AGCCTCGAGAATTCGATGCA	HBe RT-PCR, forward
Primer 29	ATCTAGAAGATCTCGTACTG	HBe RT-PCR, reverse
Primer 30	GATTCCTAGGACCCCTTCT	HBs RT-PCR, forward
Primer 31	CGATAACCAGGACAAGTTG	HBs RT-PCR, reverse
Primer 32	CGATGCCCCTATCCTATCAA	Pol RT- PCR, forward

Primer 33	AAAGACAGGTACAGTAGAAGA	Pol RT- PCR, reverse
Primer 34	CAAA GAA TTCATGGCTGCTCGGTTGTGC	HBx RT-PCR, forward
Primer 35	CCAA GGG CCCGGCAGAGGTGAAAAAGTTGC	HBx RT-PCR, reverse
Primer 36	TCTATTTCCGGTGAATTCGCCACCATGGATTACAA GGATGACGACGATAAGTAATCAGGAATTGGAAAT	RNF20-Flag to pLVX-G, forward
Primer 37	GGGAGAGGGGCGGGATCCTCAACCAATGTAGAT GCG	RNF20-Flag to pLVX-G, reverse
Primer 38	CTAACTTTGGCTCTTCACCT	Amplicon at 0.5 Kb, forward
Primer 39	GATGGAGAAAGAGAAAGGGA	Amplicon at 0.5 Kb, reverse
Primer 40	TCGCCAGTGCTTTTTCTTTT	Amplicon at 3.5 Kb, forward
Primer 41	GTTGGGGGATGATGAAAATG	Amplicon at 3.5 Kb, reverse
Primer 42	ATGGCTCATGCCTGTAATCC	Amplicon at 10 Kb/ Total DNA, forward
Primer 43	CAGCCTCCCAAGTAGCTGAG	Amplicon at 10 Kb/ Total DNA, reverse
Primer 44	CCTCCCAGAGAACAAACAGC	Amplicon at 50 Kb/ Input, forward
Primer 45	GGTTCGGGTAGGTTTTTCCT	Amplicon at 50 Kb/ Input, reverse
Primer 46	GCTCAGCTAGTCTTCTTCCTC	Amplicon for Uncut, forward
Primer 47	CTTAGAGGTTCTGGCAAGGAG	Amplicon for Uncut, reverse
Primer 48	AGGTGAAGGTCGGAGTCAAC	RT-PCR for h*GAPDH*
Primer 49	CGCTCCTGGAAGATGGTGAT	RT-PCR for h*GAPDH*

Table S3. Antibodies used in this study

Antibodies	Source
Rabbit α-RPA32 serum	Custom-made
Mouse α-RPA32	Santa Cruz, sc-271578
Rabbit α-phosphor-Serine 33, RPA32	NOVUS, NB100-544
Rabbit α-phosphor-Serine 4/8, RPA32	Bethyl, A300-245A
Rabbit α-phosphor-Serine 139, H2AX	Cell Signalling, 9718S
Mouse α-phosphor-Serine 139, H2AX	Millipore, 05-636
Rabbit α-phosphor-Serine 343, NBS1	Epitomics, 2194-1-1
Rabbit α-NBS1	NOVUS, NB100-143
Mouse α-alpha-Tubulin	Sigma, T6074
Mouse α-BrdU	Changdao (Shanghai), M-0042
Rabbit α-RAD51	Proteintech, 14961-1-AP
Rabbit α-CUL4A	Proteintech, 14851-1-AP
Mouse α-HBx	Abcam, ab235
Rabbit α-DDB1	Epitomics, 3821-1-1
Rat α-HA	Roche, 11867423001
Rabbit α-Flag	Hua'an (Hangzhou), custom-made
Mouse α-MYC	Roche, 11667149001
Rabbit α-WDR70	Bethyl, A301-871A-1
Mouse α-mono-ubiquitinated H2B	Millipore, 05-1312
Mouse α-H2B	Chemicon, ab1623
Mouse α-H3	Millipore, 05-1341
Mouse α-dimethyl H3K4	Millipore, 05-1338
Mouse α-trimethyl H3K4	Millipore, 05-1339
Rabbit α-dimethyl H3K9	Upstate, 07-212
Mouse α-trimethyl H3K9	Millipore, 05-1250
Mouse α-trimethyl H3K27	Millipore, ABE44

Rabbit α-dimethyl H3K79	Millipore, 04-835
Mouse α-trimethylH4K20	Millipore, 07-463
Mouse α-dimethyl H4K20	Upstate, 07-031
HRP-conjugated α-mouse IgG	DAKO, P0260
HRP-conjugated α-rabbit IgG	DAKO, P0448
FITC- conjugated α-mouse IgG	Sigma, F0257
CY3- conjugated α-rabbit IgG	Sigma, C2306
Rabbit α-RNF20	Bethyl, A300-714A
Mouse α-HBc	Abcam, ab8637
Mouse α-HBs	Absin, abs128707

Table S4. The pathology and aetiology of the HCC and non-HCC liver biopsies

Patient No.	**Clinical diagnosis**	**Tumor differentiation**	**Major aetiology**	**uH2B stains**
1	HCC	high	HBV	+
2	HCC	high	HBV	+/−
3	HCC	high	HBV	−
4	HCC	high	HBV	−
5	HCC	high	HBV	−
6	HCC	high	HBV	−
7	HCC	high	HBV	−
8	HCC	high	HBV	−
9	HCC	high	HBV	−
10	HCC	moderate	HBV	+++
11	HCC	moderate	HBV	−
12	HCC	moderate	HBV	−
13	HCC	moderate	HBV	−
14	HCC	moderate	HBV	−
15	HCC	moderate	HBV	−
16	HCC	moderate	HBV	−

17	HCC	moderate	HBV	−
18	HCC	moderate	HBV	−
19	HCC	poor	HBV	+++
20	HCC	poor	HBV	−
21	HCC	poor	HBV	−
22	HCC	poor	HBV	−
23	HCC	poor	HBV	−
24	HCC	poor	HBV	−
25	HCC	poor	HBV	−
26	HCC	poor	HBV	−
27	HCC	poor	HBV	−
28	HCC	high	Non-viral, alcohol	++
29	HCC	high	Non-viral	++
30	HCC	high	Non-viral	+/−
31	HCC	high	Non-viral	−
32	HCC	high	Non-viral, alcohol	−
33	HCC	high	NASH	−
34	HCC	high	Non-viral	−
35	HCC	moderate	Non-viral, alcohol	++
36	HCC	moderate	Non-viral	++
37	HCC	moderate	Non-viral	++
38	HCC	moderate	Non-viral	−
39	HCC	moderate	Non-viral	−
40	HCC	moderate	Non-viral	−
41	HCC	moderate	HCV	−
42	HCC	poor	Non-viral	+++
43	HCC	poor	Non-viral	+++
44	HCC	poor	Non-viral	++
45	HCC	poor	Non-viral, alcohol	+++
46	HCC	poor	Non-viral	++

47	HCC	poor	Non-viral, alcohol	++
48	HCC	poor	Non-viral	+
49	HCC	poor	Non-viral	−
50	HCC	poor	Non-viral	−
51	HCC	poor	Non-viral	−
52	HCC	poor	Non-viral	−
53	Non-HCC, cirrhosis		HBV	++
54	Non-HCC, NA		HBV	+
55	Non-HCC, hepatic cyst		HBV	++
56	Non-HCC, NA		HBV	+
57	Non-HCC, NA		HBV	+
58	Non-HCC, invisive tumor from other tissue		Non-viral	+++
59	Non-HCC, adiposis hepatica		Non-viral, NASH	++
60	Non-HCC, Gallstones and cholecystitis		Non-viral	+++
61	Non-HCC, adiposis hepatica		Non-viral, NASH	+++
62	Non-HCC, adiposis hepatica		Non-viral, NASH	+++
63	Non-HCC, adiposis hepatica		Non-viral, NASH	+++
64	Non-HCC, Hepatic neuroendocrine tumor		Non-viral	+++
65	Non-HCC, hepatic abscess		Non-viral	+++
66	Non-HCC, hepatitis		HCV	+++

	C			
67	Non-HCC, NA		Non-viral	+++
68	Non-HCC, invisive tumor from other tissue		Non-viral	+++
69	Non-HCC, cirrhosis		Non-viral	+++
70	Non-HCC, cirrhosis		HCV	+++
71	Non-HCC, NA		Non-viral	+++
72	Non-HCC, hepatic hemangioma		Non-viral	+++
73	Non-HCC, NA		Non-viral	+

Non-HCC liver tissues were obtained from liver biopsy specimens of patients with various liver diseases；NASH, non-alocholic steatohepatitis.